The 2009 IEEE/RSJ International Conference on
Intelligent Robots and Systems
October 11-15, 2009 St. Louis, USA

Adaptive Immune System Inspired Perimeter Patrol Control Strategy

Ruoting Yang, *Member, IEEE*, Sharon Bewick, Mingjun Zhang, *Senior Member, IEEE,*

William R. Hamel, *Fellow, IEEE,* Tzyh-Jong Tarn, *Fellow, IEEE*

Abstract— **This paper investigates a perimeter patrol control problem in which multiple agents travel back and forth defending a border. A decentralized control inspired from the adaptive immune system TH1/TH2 differentiation mechanism has been proposed. The resulting patrol control exhibits robustness under adversarial conditions. This is primarily because the motion period can be arbitrary, which makes it difficult for intruders to find weak spots for attack. Moreover, this immuno-inspired control can avoid collision and automatically recover from agent failure.**

I. Introduction

THE use of large scale distributed unmanned agents, such as aircrafts, and ground or underwater vehicles, is becoming a central theme of military force protection for conducting cooperative tasks, such as military base and homeland security patrolling. Patrolling is a common mission in which multiple agents cooperatively travel around an asset of high interest and strike any hostile intrusion attempts. In addition to force protection, patrol strategy has many potential industry applications such as search engine operation[1], failure detection[2], surveillance [3], and coordination of robotic fish [4].

Conventionally, patrol tasks are implemented in a centralized framework whereby a central station gathers global information, and designs motion for every agent involved. Centralized patrol control, however, relies on global optimization and communication, thus computational complexity grows sharply as the number of agents increases. In contrast, decentralized control relies on each agent using an identical control mechanism corresponding to local information. Different patrol strategies have been widely discussed and compared [5] in open literature; however, most papers focus on evaluating the performance of the patrol strategies, instead of designing the controls themselves. In this paper, we propose a decentralized control strategy for cooperative patrolling. We then evaluate the control strategy following robustness performance criteria.

The performance of patrol strategies can be evaluated based on both optimality with respect to design goals and robustness. Chevaleyre [6], for example, compared idleness time in cyclic strategies and partition based strategies, where each agent patrols inside its own non-overlapping(disjoint) region. The conclusion in [6] was that cyclic strategies are preferred as long as the patrol path does not contain a long edge. Elmaliach, et al. [7] investigated a partition-based patrol for a long fence. They examined synchronized motion for both disjoint (synchronized scheme) and overlapping (synchronized overlap scheme) partitions and concluded that the use of an overlap improves the uniformity of visitation frequency without sacrificing average or under-bounding frequencies except at the edges of the fence. Unfortunately, both synchronized and synchronized overlap schemes always visit any given point at fixed frequency, thus the adversary can easily penetrate the border by determining the patrol frequency over a short observation period. Agmon et al. [8] considered the problem of fixed frequency visitation in the presence of an adversary and proposed three patrol algorithms based on random walk. Unfortunately, Machado et al. [5], has shown that random patrol strategies have the worst performance in terms of idleness time.

There are three requirements that we use to design our perimeter patrol scheme.

1. Each agent switches its direction when it meets either another agent or a boundary
2. Each agent only knows the distance to its neighbors, but has no large scale knowledge of the overall agent distribution within the system
3. Motion pattern cannot be easily detected

Although the perimeter patrol scheme shares some similarity with formation control [9-11] or circular pursuit [12, 13], perimeter patrol control drives every agent moves back and forth so as to defend a border against intrusion, instead of stabilizing in a fixed topological structure or synchronously rotating in a circular path.

In this paper, we propose an adaptive immune system TH1/TH2 (T-helper 1 lymphocyte/T-helper 2 lymphocyte) differentiation mechanism [14] inspired control to tackle the perimeter patrol problem. During the adaptive immune response, TH1 and TH2 cells self-reinforce and mutually inhibit each other to rapidly switch between two dominant pathways. Detailed information about the TH1/TH2 cellular differentiation mechanism is presented in the next section. Generally speaking, this control model can be seen as a natural mechanism for generating a virtual spring.

As shown in Figure 1, this virtual spring mechanism can behave as a decision-making block to achieve two opposite

R. Yang, S. Bewick, M. Zhang, and W. Hamel are with Department of Mech., Aero. and Biom. Eng., The University of Tennessee, Knoxville, TN, USA. (Email: mjzhang@utk.edu.) T.J. Tarn is with Department of Electrical and Systems Engineering, Washington University in St. Louis.

states robustly and rapidly. Specifically, in the patrol problem, the virtual spring can drag the agent eventually causing it to turn around when the distance to the neighbor is beyond a critical threshold. Despite superficial similarities, when compared to the spring-mass-spring model, our patrol strategy shows a superior ability to automatically recover from agent failure. In addition, it is easy to create a complex deterministic motion pattern that appears random, even to adversaries with reasonably advanced cognitive skills.

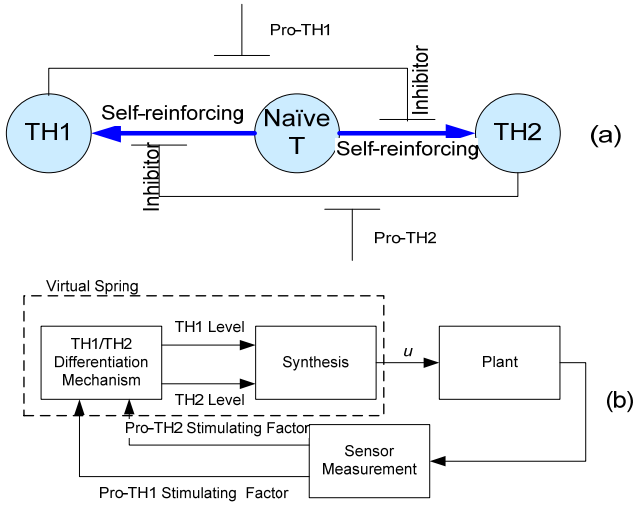

Figure 1. Control schematic of the TH1/TH2 differentiation mechanism. (a) TH1 and TH2 cells self-reinforce by stimulating Naïve T cells to convert into a similar cell type, while mutually inhibiting production of the other cell type. The external stimulating signals, Pro-TH1 and Pro-TH2 counteract the inhibitor effect. (b) The TH1/TH2 differentiation block determines the appropriate TH1/TH2 concentrations based on external stimulating factors from sensor measurements. The decision-making block considers both TH levels and sends a final decision for the control to the plant.

II. Adaptive Immune Response and TH1/TH2 Differentiation Mechanism

Adaptive immune responses play a key role in human immune defense against both extracellular (some bacteria and parasites) and intracellular (some bacteria and viruses) pathogens. The adaptive immune response adjusts the concentration of TH1/TH2 lymphocytes to drive two types of immune pathways, one designed to eliminate extracellular pathogens, and the other to defend against intracellular pathogens. Misuse or overactivation of either pathway leads to tissue injury.

As illustrated by the control diagram in Figure 2, contaminated host cells can be regarded as a plant, while APCs (antigen presenting cells) function as sensors actively measuring the pathogen load, and providing inputs to the TH1/TH2 differentiation mechanism that acts as the control. The TH1/TH2 control then responds to sensor (APC) feedback by secreting a cytokine profile which can stimulate the actuator to produce appropriate combinations of effector cells (macrophages, B cells, mast cells, and eosinophils). Finally, the effector cells themselves regulate the pathogen load by digesting and killing the pathogens.

The control block (ie the TH1/TH2 differentiation step [15-17]) is illustrated in more detail in Figure 3. APCs secrete cytokines IL-12 and IL-6 to assist naïve CD4+ T helper lymphocytes in differentiating into TH1/TH2 lymphocytes. TH1 cells then secrete the cytokine IFN-γ (Interferon - gamma)[18] which promotes a type 1 pathway to fight against intracellular pathogens and cancerous cells. In contrast, TH2 cells secrete the cytokine IL-4 which stimulates a type 2 pathway (including up-regulation of antibody production) to fight against extracellular organisms [16]. In addition, IFN-γ and IL-4 inhibit each other, thereby repressing differentiation along the alternate pathway.

The TH1/TH2 differentiation mechanism can be generalized by the model illustrated in Figure 1. TH1 cells secrete IFN-γ to inhibit Naïve T cell differentiation into TH2 cells. In keeping with other similar biological models, we will describe this process using a Hill function [19]

$$f_1(\mathrm{TH}_1) = \gamma_1^p / (\gamma_1^p + \mathrm{TH}_1^p), \quad (1)$$

where TH_1 is the concentration of TH1 cells in the immune system and γ_1 is TH1 concentration at which inhibition of TH2 production is halved. The cooperativity factor p is used to determine the maximum slope of the inhibitory response as a function of TH1 levels. Higher values of p give a more digital response.

Similarly, the inhibitory effects of TH2 cells on TH1 differentiation can be modeled as follows,

$$f_2(\mathrm{TH}_2) = \gamma_2^p / (\gamma_2^p + \mathrm{TH}_2^p) \quad (2)$$

where TH_2 is the concentration of TH2 cells in the immune system and γ_2 is TH2 level at which inhibition of TH1 production is halved.

The stimulation signals, Pr_1 and Pr_2, arise from the IL-12 and IL-6 cytokine concentrations respectively, both of which are derived from APCs. IL-12 and IL-6 counteract the inhibitory effect of TH1 and TH2 cells.

$$\mathrm{Pr}_1 = g_1(d_1) = \lambda_1 d_1^q / (\sigma_1^q + d_1^q), \quad (3)$$

$$\mathrm{Pr}_2 = g_2(d_2) = \lambda_2 d_2^q / (\sigma_2^q + d_2^q), \quad (4)$$

where d_1 and d_2 stand for the levels of IL-12 and IL-6, respectively. The stimulating effects of these cytokines occur at maximum rates of λ_1 for IL-12 and λ_2 for IL-6, with half-maximum thresholds at σ_1 and σ_2 respectively. The self-reinforcing effects of TH1 and TH2 can be described as constant process with rates α_1 and α_2.

Thus, the TH1/TH2 differentiation mechanism in Figure 1 can be described as follows,

$$\frac{d\mathrm{TH}_1}{dt} = [\alpha_1 + g_1(d_1)] \cdot f_2(\mathrm{TH}_2) - \mu \mathrm{TH}_1, \quad (5)$$

$$\frac{d\mathrm{TH}_2}{dt} = [\alpha_2 + g_2(d_2)] \cdot f_1(\mathrm{TH}_1) - \mu \mathrm{TH}_2, \quad (6)$$

Figure 4 (Left) illustrates a toggle switch phenomenon, called bi-stability, between the two pathways (TH1 vs TH2) [20-22]. The exclusive presence of IL-6 causes the TH2 pathway to dominate, while the exclusive presence of IL-12 causes the TH1 pathway to dominate.

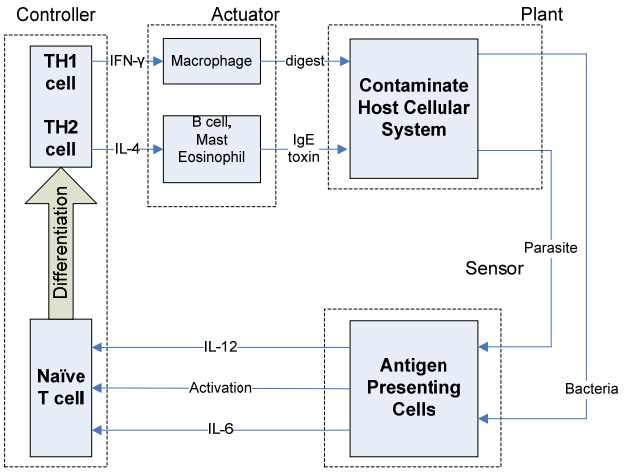

Figure 2. Control diagram of the adaptive immune response. Intra- and extra-cellular pathogens form the control plant block, while APCs detect the pathogen load as a sensor and delivery a decision to the control block - TH1/TH2 differentiation mechanism. The control secretes a cytokine profile to activate an appropriate combination of macrophages, B cells, mast cells, and eosinophils, which go on to kill the pathogens.

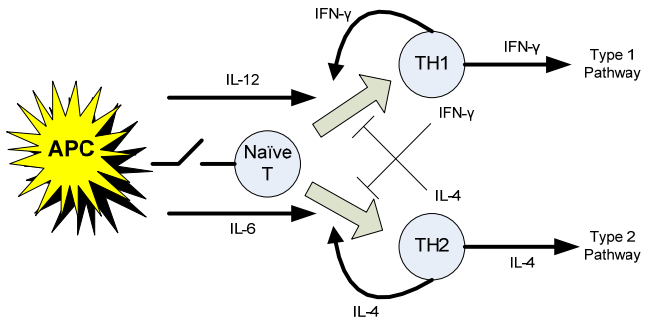

Figure 3. Illustration of the TH1/TH2 differentiation mechanism. APC cells activate naïve T cells to differentiate into either TH1 or TH2 cells. Both cell subsets secrete cytokines to promote their own differentiation pathway while simultaneously inhibiting the other.

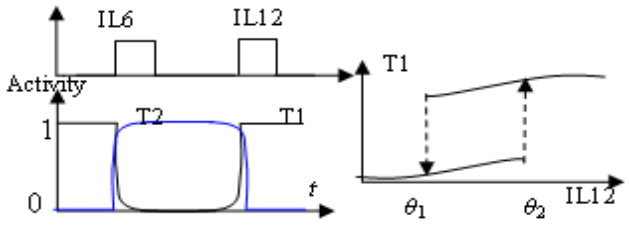

Figure 4 Bistabilty and hysteresis in the TH1/TH2 differentiation mechanism. (Left) The process toggles between a TH1-on state and a TH2-on state in response to trigger stimuli IL12 and IL6. It ensures no intermediate state for both TH1-on and TH2-on. (Right) Hysteresis. When the IL12 signal accumulates to a critical upper threshold, $\theta 2$, the TH1 state switches ON, and only switches to OFF again once the IL12 signal has dissipated to a level below the lower threshold, θ_1.

Figure 4 (Right) shows another interesting characteristic - hysteresis [22]. When the IL12 signal accumulates to a critical threshold θ_2, TH1 differentiation is activated. However, even when the IL12 signal dissipates to levels below θ_2, TH1 differentiation is not be deactivated immediately. Instead, the IL-12 signal must fall below the lower threshold θ_1 in order to initiate TH1 differentiation deactivation. The hysteresis phenomenon arises from the supercritical Hopf bifurcation of the center equilibrium.

As shown in Figure 1(b), the TH1/TH2 differentiation mechanism can be easily applied to a control system. As a result of its combination of mutual inhibition and self-reinforcement, the TH1/TH2 differentiation block can robustly and rapidly determine the appropriate TH1/TH2 concentrations based on external stimulating factors from the bio-sensor measurements. The synthesis block then determines the control by combining the TH1/TH2 levels using some generic function

$$u = L(\mathrm{TH}_1, \mathrm{TH}_2)\,. \tag{7}$$

This function can be either a complex nonlinear function or simple linear combination of TH1 and TH2 levels.

In a perimeter patrol control problem, a single agent receives stimuli that promote either moving-to-left or moving-to-right. These stimuli are analogous to cells in the immune system which support either TH1 or TH2 differentiation. Just as the immune system integrates the TH1 and TH2 cell concentrations in order to make a final decision on effector cell output, the patrol control agent must integrate left vs. right stimuli in order to make a final decision on its speed and direction of travel. With respect to patrol control, for example, drifting too far from its neighbor on the right would give a 'move-to-the-right' stimulus, while drifting too far from its neighbor on the left would give a 'move-to-the-left' stimulus. With this simple, yet reasonably practical decision-making mechanism, an agent can make a rapid and robust decision as to whether it should move forward or turn around in order to minimize the distance between itself and its nearest neighbors. This is exactly what a perimeter patrol control needs.

III. TH1/TH2 DIFFERENTIATION INSPIRED PERIMETER PATROL

A. Perimeter Patrol Problem statement

Assume N agents travel along an open polygon, e.g., a two-ended fence. Each agent will change the direction of its motion when it meets the end points or another agent. Without loss of generality, the agents are considered as point particles patrolling along a straight L-length fence with left/right end-points at x_{N+1} / x_0, respectively. The positions of the agents are defined orderly as $x_0 > x_1 > x_2 > \ldots > x_N > x_{N+1}$ in Euclidean space R.

Two agents in close proximity to the end-points have only one moving neighbor, while all others possess two neighbors. The neighboring set of agent i contains only agent $i+1$ and $i-1$. Agent 1 has a fixed neighbor at x_0, while agent N has a fixed neighbor at x_{N+1}. Each agent is able to detect its neighbors within the detection range D: $\{x|\ |x - x_i| < r_D\}$. Assume that the adversary will choose to penetrate through the weakest spot. This means that if the distance between two adjacent agents is greater than r_D, the probability of penetration increases sharply and then grows with distance for $|x_i - x_{i\pm1}| > r_D$. Furthermore, assume that the fence is very long, and that the number of agents is always insufficient keep all spots within detection range, i.e., $2Nr_D < L$.

Otherwise, the agents would only need to guard equidistantly between the extremities.

Without loss of generality, kinetics of agent i can be described by a particle model:

$$\dot{x}_i = u_i \,, \tag{8}$$

where x_i stands for the position of the agent i, and u_i represents the speed control to the agent.

The agent patrol control uses the mutual inhibitory mechanism inspired by TH1/TH2 differentiation. Each agent moves in a manner dependent on the distances between itself and its two nearest neighbors. As shown in Figure 5, the multiple agent patrol strategy constructs a mutual inhibitory multi-agent chain.

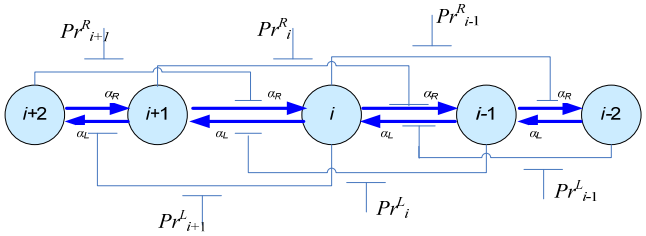

Figure 5 The mutual inhibitory multi-agent chain. Agent $i-1$ affects agent i's velocity of to the left; while the agent $i+1$ affects agent i's velocity to the right.

Similar to the single agent case, for agent i, the kinetic model is described as follows,

$$\dot{x}_i = v_i^R - v_i^L \,, \tag{9}$$

$$\dot{v}_i^R = \frac{\alpha_i^R + \mathrm{Pr}_i^R}{1+(v_i^L)^p} - \mu_i v_i^R \,, \tag{10}$$

$$\dot{v}_i^L = \frac{\alpha_i^L + \mathrm{Pr}_i^L}{1+(v_i^R)^p} - \mu_i v_i^L \,, \tag{11}$$

where v_i^R and v_i^L are decision factors for agent i corresponding to movement to the right and movement to the left respectively. The positive coefficients α_i^R and α_i^L represent the self-reinforcement rates, while μ_i denotes the degradation rate for agent i. The control inputs Pr_i^R and Pr_i^L can be determined as a function of the distance between agent i and its left or right neighbor. The control can be formulated as

$$\mathrm{Pr}_i^R = \frac{\lambda_i^R \,|\, x_i - x_{i+1} \,|}{\sigma_i^R + |\, x_i - x_{i+1} \,|} \text{ and } \mathrm{Pr}_i^L = \frac{\lambda_i^L \,|\, x_i - x_{i-1} \,|}{\sigma_i^L + |\, x_i - x_{i-1} \,|} \tag{12}$$

a) Stability Analysis

The equilibriums of (9)-(12) can be determined by the following equations, for i =1, …, N,

$$v_i^R = v_i^L \tag{13}$$

$$\alpha_i^R + \frac{\lambda_i^R (x_{i-1} - x_i)}{\sigma_i^R + (x_{i-1} - x_i)} = \mu_i v_i^R \left[1 + (v_i^L)^p\right] \tag{14}$$

$$\alpha_i^L + \frac{\lambda_i^L (x_i - x_{i+1})}{\sigma_i^L + (x_i - x_{i+1})} = \mu_i v_i^L \left[1 + (v_i^R)^p\right] \tag{15}$$

If $\alpha_i^R = \alpha_i^L = \alpha$, $\lambda_i^R = \lambda_i^L = \lambda$, and $\mu_i = \mu$, then

$$x_i = (\sigma_i^R x_{i+1} + \sigma_i^L x_{i-1})/(\sigma_i^R + \sigma_i^L) \,. \tag{16}$$

When $\sigma_i^R = \sigma_i^L = \sigma$, it implies that $x_i = (x_{i-1} + x_{i+1})/2$, and thereby,

$$x_i = [(N-i)x_{N+1} + ix_0]/N \tag{17}$$

This means that $v_i^R = v_i^L = v_i$ can be solved by

$$v_i + v_i^{p+1} = \bar{\Delta} = \frac{\alpha}{\mu} + \frac{\lambda(x_0 - x_{N+1})}{\mu(N\sigma + x_0 - x_{N+1})} > 0 \,. \tag{18}$$

If p = 2, then there are three solutions for v_i. These are

$$\frac{\bar{\Omega}}{6} - \frac{2}{\bar{\Omega}}, -\frac{\bar{\Omega}}{12} + \frac{1}{\bar{\Omega}} \pm j\frac{\sqrt{3}}{2}\left(\frac{\bar{\Omega}}{6} + \frac{2}{\bar{\Omega}}\right) \tag{19}$$

where $j = \sqrt{-1}$ and $\bar{\Omega} = \left(108\bar{\Delta} + 12\sqrt{12 + 81\bar{\Delta}^2}\right)^{1/3}$. We again note that only the real solution $v_i = \bar{\Omega}/6 - 2/\bar{\Omega} \geq 0$ is feasible. This leads to $\bar{\Omega} \geq 2\sqrt{3}$. For each agent, the Jacobian matrix with respect to the equilibrium $(0, v_i, v_i)$ can be written as

$$\begin{bmatrix} 0 & 1 & -1 \\ \bar{a}_{21} & -\mu & \bar{a}_{23} \\ \bar{a}_{31} & \bar{a}_{32} & -\mu \end{bmatrix} \tag{20}$$

where $\bar{a}_{31} = -\bar{a}_{21} = \dfrac{\lambda v_i}{\bar{\Delta}\sigma[1 + (x_0 - x_{N+1})/(N\sigma)]^2} > 0$, and $\bar{a}_{23} = \bar{a}_{32} = \dfrac{-2v_i^3}{\bar{\Delta}^2}\left(\alpha + \dfrac{\lambda}{1 + (N\sigma)/(x_0 - x_{N+1})}\right) < 0$.

The Jacobian has three eigenvalues: $\bar{a}_{23} - \mu < 0$, $\dfrac{-(\mu + \bar{a}_{23}) \pm \sqrt{(\mu + \bar{a}_{23})^2 - 8\bar{a}_{31}}}{2}$. Thus,

1. If $\mu_i > -\bar{a}_{23}$, then the equilibrium is stable and agent i converges to $x_i = [(N-i)x_{N+1} + ix_0]/N$.
2. If $\mu_i < -\bar{a}_{23}$ and $(\mu_i + \bar{a}_{23})^2 - 8\bar{a}_{31} > 0$, then the equilibrium is unstable and agent i diverges.
3. If $\mu_i < -\bar{a}_{23}$ and $(\mu_i + \bar{a}_{23})^2 - 8\bar{a}_{31} < 0$, then the equilibrium will have a Hopf bifurcation and agent i will oscillate.

b) Simulation Results

When the stimulating signals are distinct for each agent, the patrol pattern will appear very different. For example, assume $\sigma^L = \sigma^R = [2.5, 4.5, 2.5]$, Figure 6 presents an overlap long periodic patrol scheme. The oscillation period is very long, (more than 200 s). The visitation frequency of all points is 0.12 Hz at the center and 0.08 Hz at the region close to extremities. Figure 7 shows a non-overlap periodic patrol scheme in which each agent covers one third of the fence. The visiting frequency is the same as the prior scheme, uniformly distributed at 0.12 Hz. Figure 8 illustrates another overlap periodic patrol scheme, for $\sigma^L = \sigma^R = [2.4, 3.36, 2.4]$.

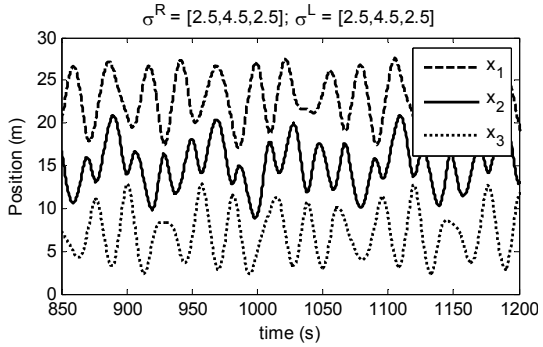

Figure 6. Three agents conduct overlap long periodic patrol between two boundaries, when $\mu_i = 0.8$, and $\sigma^R = \sigma^L = [2.5, 4.5, 2.5]$. The three curves again represent the motion trajectories of the three agents.

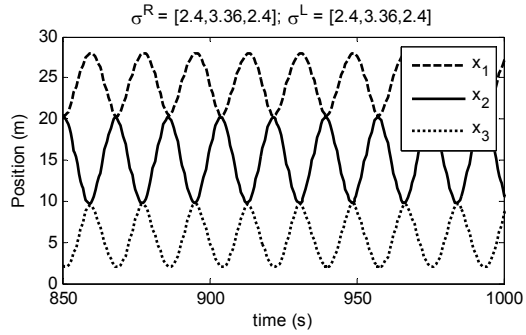

Figure 7. The agents conduct a non-overlap periodic patrol strategy. The agents divide the patrol path into three parts and patrol their respective regions at the same frequency.

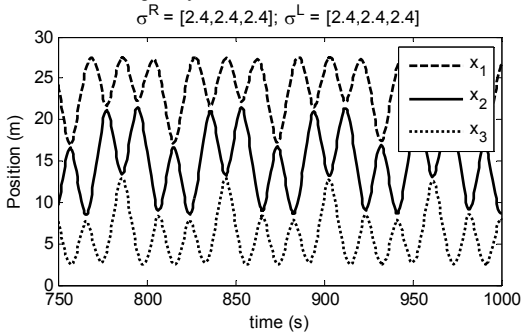

Figure 8. Three agents conduct overlap periodic patrol. The patrol regions of the three agents overlap, but the agents do not collide. The motion pattern appears more complex than the corresponding pattern for non-overlap periodic patrol, but simpler than the pattern for non-overlap long periodic patrol.

Robustness is another important issue for any patrol control scheme, especially when one or more agents stop moving. In this case, the other agents must continue perimeter patrol, and automatically enlarge their patrol ranges to cover the area belonging to the ill-functioning agents.

Figure 9 illustrates the automatic recovery of the patrol control scheme for a situation in which the middle agent (agent 2) suddenly stops around marker 10 m. Agent 1 and agent 3 then enlarge their ranges to cover the whole fence. Because the position of agent 2 becomes constant, it functions as an end-point to the neighbors. As a result, agent 1 and agent 3 will patrol as if they were single agents performing according to the single agent model. When agent 2 recovers, after a short transition period, the whole group resumes its original behavior as if none of the agents had ever malfunctioned.

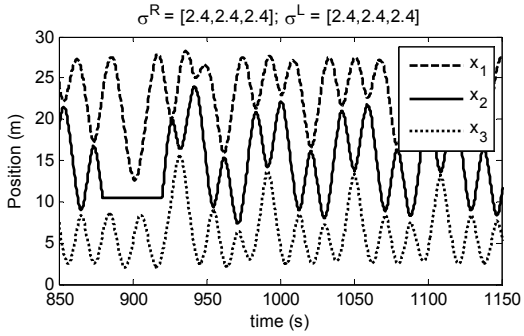

Figure 9. Illustration of failure recovery. The curves stand for the motion trajectories of the three agents from top to bottom. The agents first conduct the overlap periodic patrol. Agent 2 then stops due to obstacles from 880 s to 920 s, while the other two agents continue patrolling and extend their patrol ranges. When agent 2 recovers, the agents resume their patrol strategy.

IV. Discussions and Conclusions

A. Comparison to robustness of three patrol patterns

In Section III, three patrol patterns have been created by the TH1/TH2 differentiation inspired control.

1. overlap non-periodic motion (Figure 6)
2. non-overlap periodic motion (Figure 7)
3. overlap periodic motion (Figure 8)

For all strategies, the visiting frequencies at every point are uniformly distributed. Thus, the efficiencies with respect to mean visiting frequency [23] have no significant difference. However, in an adversary setting, robustness performance of preventing penetration becomes more important. We define the following criteria for the performance of penetration prevention:

1. Mean Max Gap: The average maximum distance between agents.
2. Variance of Weakest Points: Variance of the midpoints of the maximum gap between agents.

Strategy 1 has the best performance in terms of mean max gap (12.7). Strategy 3, on the other hand, has the worst mean max gap (14.1) of the three patrol scheme categories.

As suggested earlier, however, synchronized patrol always visits points at the same frequency. The adversary can therefore easily penetrate the fence. As a result, we will consider the variance of weakest points. The weakest points of strategy 1 are widely distributed with variance 35.4. The weakest points of strategy 2 are uniformly distributed in $[10, 12]$ and $[18, 20]$, with a variance of 18.8. The weakest points of strategy 3 are almost uniformly distributed in $[5, 25]$ with a variance of 30.2.

In terms of robustness criteria, we can conclude that overlap non-periodic strategies have the best performance among the three patrol patterns considered.

B. Comparison to spring-mass-spring model

The oscillation behavior is often analogous to the spring-mass-spring model. However, the patrol strategy based on the spring-mass-spring model cannot recover after temporary failure. Consider a horizontal spring-mass-spring

model,

$$m\ddot{x} = -(k_1 + k_2)(x - (x^R - x^L)/2), \quad (21)$$

where m stands for the mass and k_1, k_2 are spring constants. x^R and x^L denote right and left boundaries. x is the displacement from the left boundary.

This is a simple harmonic motion; however, if the mass is stopped by an obstacle for a short time, then as shown in Figure 10, the oscillation magnitude will not recover. As a result, the spring-mass-spring model lacks robustness to temporary failure, while our approach demonstrates the capability to recover after agent malfunction. This unique capability leads to an advantage that is crucial if the control scheme is to be used in decentralized patrol control. Specifically, no supervised control is necessary to reset the patrol scheme when agent failure and recovery occurs.

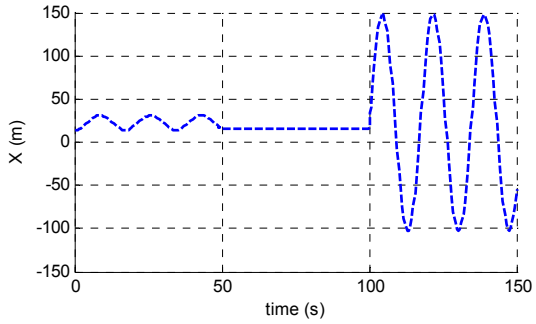

Figure 10 The spring-mass-spring model-based patrol method fails to recover after the agent is stopped by an obstacle for a short time. The spring control model has to reset the agents' positions when agent failure and recovery occurs. In contrast, the "virtual spring" control – TH1/TH2 differentiation control exhibits superior robustness in the face of agent failure and recovery.

This paper studies perimeter patrol control problem that drive multiple agents back and forth along a path with two endpoints. A patrol control inspired from the TH1/TH2 differentiation mechanism that occurs during the adaptive immune response has been applied. This decentralized control mechanism is simple, yet complex enough to be useful for military force protection and many other industry applications including the functioning of search engines, failure detection and robotics. Three typical patrol behaviors created by the immuno-inspired control have been evaluated, and overlap non-periodic patrol strategy shows better performance than the others in terms of robustness and stability. In addition, the immuno-inspired method can automatically recover from agent failure.

REFERENCES

[1] J. Cho and H. Garcia-Molina, "Synchronizing a Database to Improve Freshness," in *Proceedings of 2000 ACM International Conference on Management of Data*, 2000.

[2] R. d. C. Andrade, H. T. Macedo, G. L. Ramalho, and C. A. G. Ferraz, "Distributed mobile autonomous agents in network management," in *Proceedings of International Conference on Parallel and Distributed Processing Techniques and Applications*, 2001.

[3] K. Williams and J. Burdick, "Multi-robot boundary coverage with plan revision," in *Proceedings of IEEE International Conference on Robotics and Automation*, 2006, pp. 1716-1723.

[4] H. Sang, S. Wang, M. Tan, and Z. Zhang, "Research on Patrol Algorithm of Multiple Behavior-based Robot Fish," *International Journal of Offshore and Polar Engineering,* vol. 15, pp. 1-6, 2005.

[5] A. Machado, G. Ramalho, J. Zucker, and A. Drogoul, *Multi-agent Patrolling: An Empirical Analysis of Alternative Architectures* vol. 2581: Springer Berlin / Heidelberg, 2003.

[6] Y. Chevaleyre, "Theoretical Analysis of the Multi-agent Patrolling Problem," in *Proceedings of IEEE / WIC / ACM International Conference on Intelligent Agent Technology*, 2004, pp. 302-308.

[7] Y. Elmaliach, A. Shiloni, and G. A. Kaminka, "Frequency-based multi-robot fence patrolling," in *Technical Report MAVERICK 2008/01, Bar Ilan University, Computer Science Department, MAVERICK Group*, 2008.

[8] N. Agmon, S. Kraus, and G. A. Kaminka, "Multi-robot perimeter patrol in adversarial settings," in *Proceedings of IEEE International Conference on Robotics and Automation*, 2008, pp. 2339-2345.

[9] V. Gazi and K. M. Passino, "Stability analysis of swarms," *IEEE Transactions on Automatic Control,* vol. 48, pp. 692-697, 2003.

[10] N. E. Leonard and E. Fiorelli, "Virtual leaders, artificial potentials and coordinated control of groups," in *Proceedings of the 40th IEEE Conference on Decision and Control*, 2001, pp. 2968-2973.

[11] R. Olfati-Saber and R. M. Murray, "Consensus problems in networks of agents with switching topology and time-delays," *IEEE Transactions on Automatic Control,* vol. 49, pp. 1520-1533, 2004.

[12] J. A. Marshall, M. E. Broucke, and B. A. Francis, "Formations of vehicles in cyclic pursuit," *IEEE Transactions on Automatic Control,* vol. 49, pp. 1963-1974, 2004.

[13] R. Sepulchre, D. A. Paley, and N. E. Leonard, "Stabilization of Planar Collective Motion: All-to-All Communication," *IEEE Transactions on Automatic Control,* vol. 52, pp. 811-824, 2007.

[14] S. Romagnani, "The Th1/Th2 paradigm," *Immunology Today,* vol. 18, pp. 263-266, 1997.

[15] D. Jankovic, A. Sher, and G. Yap, "Th1/Th2 effector choice in parasitic infection: decision making by committee," *Current Opinion in Immunology,* vol. 13, pp. 403-409, 2001.

[16] P. Kidd, "Th1/Th2 Balance: The Hypothesis, its Limitations, and Implications for Health and Disease," *Alternative Medicine Review,* vol. 8, pp. 223-246, 2003.

[17] R. L. Modlin, "Th1-Th2 Paradigm: Insights from Leprosy," *J Investig Dermatol,* vol. 102, pp. 828-832, 1994.

[18] M. Jutel, M. Akdis, F. Budak, C. Aebischer-Casaulta, M. Wrzyszcz, K. Blaser, and Cezmi A. Akdis, "IL-10 and TGF-beta; cooperate in the regulatory T cell response to mucosal allergens in normal immunity and specific immunotherapy," *European Journal of Immunology,* vol. 33, pp. 1205-1214, 2003.

[19] S. Goutelle, M. Maurin, F. Rougier, X. Barbaut, L. Bourguignon, M. Ducher, and P. Maire, "The Hill equation: a review of its capabilities in pharmacological modelling," *Fundamental & Clinical Pharmacology,* vol. 22, pp. 633-648, 2008.

[20] D. Angeli, J. E. Ferrell, and E. D. Sontag, "Detection of multistability, bifurcations, and hysteresis in a large class of biological positive-feedback systems," *Proc. National Academy of Sciences,* vol. 101, pp. 1822-1827, 2004.

[21] J. E. Ferrell, "Self-perpetuating states in signal transduction: positive feedback, double-negative feedback and bistability," *Current Opinion in Cell Biology,* vol. 14, pp. 140-148, 2002.

[22] J. E. J. Ferrell and W. Xiong, "Bistability in cell signaling: How to make continuous processes discontinuous, and reversible processes irreversible," *Chaos: An Interdisciplinary Journal of Nonlinear Science,* vol. 11, pp. 227-236, 2001.

[23] Y. Elmaliach, N. Agmon, and G. A. Kaminka, "Multi-Robot Area Patrol under Frequency Constraints," in *Proceedings of IEEE International Conference on Robotics and Automation*, 2007, pp. 385-390.